Dynamic and Reversible Boundary Constraints to Guide Engineered Meniscus Microtissue Formation

Darcy D. Huang[1], Yuqi Zhang[1], Meghan E. Kupratis[1], Elizabeth R. Bernstein[1], Georgios Kotsaris[1], Robert L. Mauck[1]
[1]University of Pennsylvania, Philadelphia,
ddhuang@seas.upenn.edu

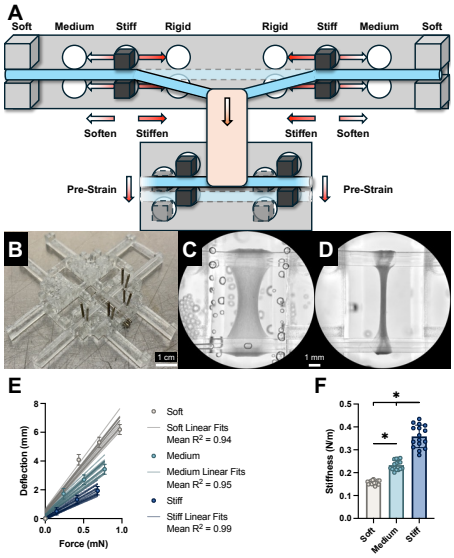

Figure 1: A) Model schematic. **B)** Assembled model. **C)** Partial and **D)** full tissue compaction. E) Deflection vs. force. **F)** Effective stiffness of the soft, medium, and stiff configurations.

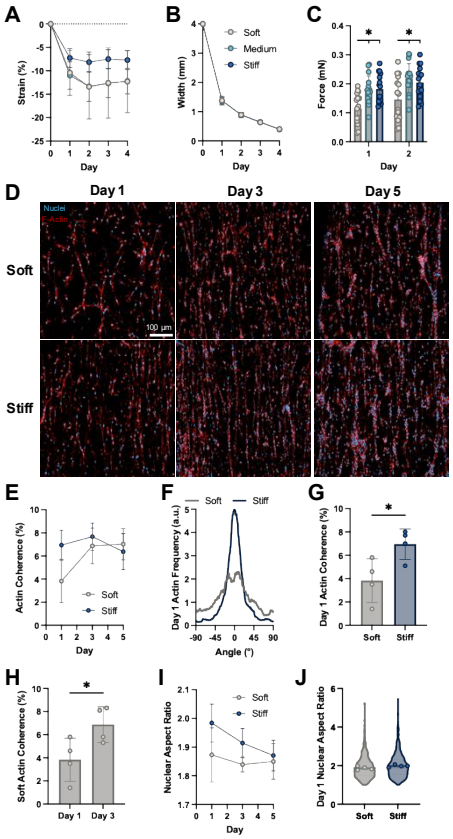

Figure 2: A) Measured strain and **B)** width over time. **C)** Force measured at Day 1 and 2. **D)** Fluorescent images of nuclei and F-actin. **E)** Actin coherence over time. **F)** Day 1 distribution of actin alignment. **G)** Day 1 actin coherence. **H)** Day 1 and 3 soft condition actin coherence. **I)** Nuclear aspect ratio over time. **J)** Day 1 nuclear aspect ratio.

Disclosures: Darcy D. Huang (N), Yuqi Zhang (N), Meghan E. Kupratis (N), Elizabeth R. Bernstein (N), Georgios Kotsaris (N), Robert L. Mauck (5-4WEB Medical)

INTRODUCTION: The meniscus is one of the most frequently injured structures in the knee,[1] and altered joint loading following injury can accelerate the development of osteoarthritis.[2] The wedge-shaped, semilunar geometry of the meniscus transforms compressive forces from the femur into circumferential tensile hoop stresses.[3] In meniscus tissue engineering, introducing tensile constraints (e.g. through mechanical anchoring at tissue boundaries) can enhance functional tissue properties.[4] However, the specific role of tensile loading in guiding intrinsic cell contractility and tissue formation remains poorly understood. Constrained microtissue models provide a powerful platform to investigate these processes by enabling real-time, *in situ* measurements of tissue-generated forces.[5] Moreover, incorporating dynamic boundary control allows for the modeling of *in vivo* processes such as developmental stiffening[6] or injury-induced softening.[3] Here, we developed a novel constrained microtissue model with dynamic and reversible stiffness and pre-strain to investigate how boundary constraints influence meniscus microtissue formation and contractility.

METHODS: Culture devices were 3D-printed in the biocompatible VisiJet SL Clear resin, and elastic strings were cast from 1:7 Sylgard 184:527 in 3D-printed ASA molds. Stainless steel rods were used to manipulate effective string bending length and position. Meniscus fibrochondrocytes (MFCs) were isolated from the medial meniscus of juvenile bovine joints. Meniscal tissues were diced into ~1 mm^3 cubes and cultured until MFCs migrated out. MFCs were used at P4. MFCs were encapsulated within 1.5 mg/mL collagen gels at 2.5 million cells/mL. Tissues were imaged using an iPhone 15 through a Zeiss Stemi 305 microscope and a Zeiss LSM 980 confocal. Statistical significance was determined using unpaired t-tests and one-way and two-way ANOVAs, with post-hoc Tukey tests where applicable. Data are reported as mean ± standard deviation. $* \; p \leq 0.05$.

RESULTS: Effective string stiffness for each configuration was determined by applying defined loads and measuring deflection, confirming a primarily linear elastic response (Fig. 1E). The medium and stiff configurations exhibited ~1.5x and ~2.3x higher stiffness, respectively, compared to the soft configuration. Under static boundary constraints, tissues were cultured for 4 days under either soft or stiff boundaries. Tissue contraction and force generation peaked at Day 2 (Fig. 2A, C). Compaction continued throughout the culture period, with minimal differences in tissue width between conditions (Fig. 2B). Force generation was significantly lower in the soft condition on Day 1 and 2 (Fig. 2C). Static boundary constraints also affected cell morphology. F-actin fibers were significantly more aligned in the stiff condition compared to the soft condition on Day 1 (Fig. 2D-G), though alignment in the soft condition increased over time and approached that of the stiff group (Fig. 2D, E, H). Both groups exhibited elongated nuclei, with no significant differences in nuclear aspect ratio (Fig. 2I, J). During dynamic culture, tissues were first primed at one stiffness for 2 days and then switched to the opposite stiffness for an additional day of culture (Fig. 3A). Based on prior observations of minimal force change between Day 2 and 3 in static culture, Day 3 force was compared to Day 2. Altering boundary stiffness induced significant changes in force generation: tissues increased force output upon softening and decreased force output upon stiffening (Fig. 3D).

DISCUSSION: Here, we developed a novel constrained microtissue model with tunable, reversible boundary stiffness and pre-strain control to evaluate how boundary constraints regulate meniscus microtissue formation and force generation. Stiff boundary conditions promoted greater contractile force and accelerated early cytoskeletal alignment, while dynamic modulation of stiffness elicited adaptive changes in tissue-generated force. These findings demonstrate that meniscus microtissues are sensitive to both the magnitude and temporal evolution of boundary stiffness. Future studies will investigate how varying pre-strain and stiffness dynamics influence meniscus microtissue formation, as well as assess molecular and matrix-level outcomes to further elucidate the mechanobiological pathways governing meniscus tissue development and adaptation.

SIGNIFICANCE/CLINICAL RELEVANCE: This platform enables the direct investigation of how boundary constraints guide meniscus tissue morphogenesis, yielding insight to inform the design of large-scale tissue constructs for meniscus repair and replacement in the clinic.

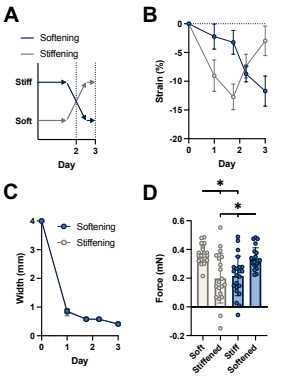

Figure 3: A) Schematic of culture conditions. **B)** Measured strain and **C)** width over time. **D)** Force measured at Day 2 and 3 with change in boundary stiffness.

REFERENCES: [1] Bilgen B+, *Adv Healthc Mater*, 2018. [2] Lohmander L+, *Am J Sports Med*, 2007. [3] Makris E+, *Biomaterials*, 2011. [4] Puetzer J+, *J Biomech*, 2015. [5] Legant W+, *Proc Natl Acad Sci U S A*, 2009. [6] Kwok B+, *Acta Biomater*, 2023.

ACKNOWLEDGEMENTS: This work was supported by an NSF GRF and the NIH (R01 AR075418).